Optical-fiber-based Mueller optical coherence tomography

Shuliang Jiao and Wurong Yu

Optical Imaging Laboratory, Department of Biomedical Engineering, Texas A&M University, 3120 TAMU, College Station, Texas 77843-3120

George Stoica

Department of Pathobiology, Texas A&M University, College Station, Texas 77843-5547

Lihong V. Wang

Optical Imaging Laboratory, Department of Biomedical Engineering, Texas A&M University, 3120 TAMU, College Station, Texas 77843-3120

Received January 8, 2003

An optical-fiber-based multichannel polarization-sensitive Mueller optical coherence tomography (OCT) system was built to acquire the Jones or Mueller matrix of a scattering medium, such as biological tissue. For the first time to our knowledge, fiber-based polarization-sensitive OCT was dynamically calibrated to eliminate the polarization distortion caused by the single-mode optical fiber in the sample arm, thereby overcoming a key technical impediment to the application of optical fibers in this technology. The round-trip Jones matrix of the sampling fiber was acquired from the reflecting surface of the sample for each depth scan (A scan) with our OCT system. A new rigorous algorithm was then used to retrieve the calibrated polarization properties of the sample. This algorithm was validated with experimental data. The skin of a rat was imaged with this fiber-based system. © 2003 Optical Society of America

OCIS codes: 120.2130, 170.0170, 170.1870, 170.4500, 260.5430.

In contrast to conventional optical coherence tomography (OCT), polarization-sensitive optical coherence tomography (PS-OCT) adds the polarization properties of the sample as a contrast mechanism.[1–6] However, practical applications of PS-OCT have been limited by the difficulty of its optical-fiber implementation. A single-mode optical fiber (SMF) alters the polarization state of the guided light because of the inherent birefringence in the fiber. The birefringence varies with the bending and twisting of the fiber during manipulation of the imaging probes, which can result in dynamic distortion in PS-OCT images. Therefore, a dynamic calibration technique is required for elimination of this effect.

Based on previous studies, a Jones matrix can be applied in PS-OCT to characterize completely the polarization properties of a sample.[2–6] If the one-way Jones or Mueller matrix of the sampling optical fiber can be determined, the polarization distortion caused by the sampling fiber can be eliminated from the PS-OCT images. Multichannel Mueller OCT can measure the Jones and Mueller matrices of a sample with a single scan and thus offer the possibility of rigorously eliminating the polarization effect of the sampling fiber. This method allows fiber-based Mueller OCT to acquire a calibrated Mueller-matrix image as rapidly as conventional OCT acquires a regular image. In this Letter we report a new rigorous calibration algorithm that was validated with experimental data and was also applied to imaging the skin of a rat.

In general, a pure retarder can be characterized by a homogeneous Jones matrix that has two orthogonal elliptical eigenvectors, each representing an eigenpolarization. When two or more linear retarders are cascaded, the overall retarder is generally elliptical unless the axes are aligned. Because of its randomly distributed birefringence along the core, a SMF should be treated as an elliptical retarder.

We first introduce the general properties of a retarder. The 2×2 Jones matrix $[\mathbf{J}(\varphi, \theta, \delta)]$ of an elliptical retarder can be expressed with three independent real parameters: $J(1,1) = \cos(\varphi/2) + i \sin(\varphi/2)\cos 2\theta$, $J(1,2) = i \sin(\varphi/2)\sin 2\theta \exp(-i\delta)$, $J(2,1) = -J^*(1,2)$, $J(2,2) = J^*(1,1)$. The fast and slow eigenvectors are $[\cos\theta, \sin\theta \exp(i\delta)]^T$ and $[-\sin\theta \exp(-i\delta), \cos\theta]^T$, respectively, where the superscript T represents a transpose operation. The angle θ is an auxiliary angle of the fast eigenvector, δ represents the phase difference between the two components of the fast eigenvector, and φ is the phase difference (retardation) between the two eigenvalues. If $\delta = 0$, the retarder is linear and θ represents the orientation of the fast axis.

The round-trip Jones matrix ($\mathbf{J}_2$) of an optical component can be calculated from its one-way Jones matrix ($\mathbf{J}_1$) according to the Jones reversibility theorem: $\mathbf{J}_2 = \mathbf{J}_1{}^T \mathbf{J}_1$. Subscripts 1 and 2 denote the one-way and round-trip parameters, respectively. Because $\mathbf{J}_2$ is transpose symmetric $[J_2(2,1) = J_2(1,2)]$, the phase difference δ_2 of $\mathbf{J}_2$ is zero, indicating that $\mathbf{J}_2$ represents a linear retarder. As a result, only two independent real parameters are needed to describe $\mathbf{J}_2$.

In a fiber-based Mueller OCT system, the incident sampling light undergoes transformation sequentially, first through the sampling fiber and the sample in forward propagation and then the sample and the sampling fiber in backward propagation. Therefore,

0146-9592/03/141206-03$15.00/0

the raw round-trip Jones matrix ($\mathbf{J}_{sf2}$) can be expressed in terms of the one-way Jones matrix of the sampling fiber ($\mathbf{J}_{f1}$) and the round-trip Jones matrix of the sample at a given imaging depth ($\mathbf{J}_{s2}$) as

$$\mathbf{J}_{sf2} = \mathbf{J}_{f1}{}^{T}\mathbf{J}_{s2}\mathbf{J}_{f1}\,. \tag{1}$$

The round-trip Jones matrix of the sampling fiber ($\mathbf{J}_{f2}$) can be calculated from the OCT signal reflected from the sample surface: $\mathbf{J}_{f2} = \mathbf{J}_{f1}{}^{T}\mathbf{J}_{f1}$.

Without discriminating between the one-way and round-trip transformations, a recently developed technique[7] used an algorithm equivalent to using $\mathbf{J}_{f2}{}^{-1}$ directly to treat $\mathbf{J}_{sf2}$. This algorithm yields $\mathbf{J}_{sf2}\mathbf{J}_{f2}{}^{-1} = \mathbf{J}_{f1}{}^{T}\mathbf{J}_{s2}(\mathbf{J}_{f1}{}^{T})^{-1}$, which is not equal to $\mathbf{J}_{s2}$ unless $\mathbf{J}_{s2}$ and $\mathbf{J}_{f1}$ are permutable. Since it does not reflect the correct physical process and it treats the sample as a pure retarder, this algorithm is unable to correctly recover the orientation of the birefringence and the diattenuation.

To eliminate the distortion, the best approach is to calculate $\mathbf{J}_{f1}$ from $\mathbf{J}_{f2}$ for each A scan. However, there are three real variables in $\mathbf{J}_{f1}(\varphi_{f1}, \theta_{f1}, \delta_{f1})$ but only two in $\mathbf{J}_{f2}(\varphi_{f2}, \theta_{f2})$. Consequently, the equation $\mathbf{J}_{f2} = \mathbf{J}_{f1}{}^{T}\mathbf{J}_{f1}$ provides only two independent relationships; therefore, $\mathbf{J}_{f1}$ can be determined only from $\mathbf{J}_{f2}$ with a free parameter.

For each $\mathbf{J}_{f2}$, we can always find a unique hypothetical linear retarder $\mathbf{J}_{fl1}$ to satisfy $\mathbf{J}_{f2} = \mathbf{J}_{fl1}{}^{T}\mathbf{J}_{fl1}$. We introduce the following matrix to reflect the free parameter:

$$\mathbf{J}_{fc1} = \mathbf{J}_{f1}\mathbf{J}_{fl1}{}^{-1}\,. \tag{2}$$

Removing the round-trip effect of $\mathbf{J}_{fl1}$ from $\mathbf{J}_{sf2}$, we obtain a new matrix $\mathbf{J}_{sc2}$:

$$\mathbf{J}_{sc2} = (\mathbf{J}_{fl1}{}^{T})^{-1}\mathbf{J}_{sf2}\mathbf{J}_{fl1}{}^{-1}\,. \tag{3}$$

Based on Eqs. (1)–(3), we have the following solution representing the general calibration algorithm in a matrix form:

$$\mathbf{J}_{s2} = (\mathbf{J}_{fc1}{}^{T})^{-1}\mathbf{J}_{sc2}\mathbf{J}_{fc1}{}^{-1}\,. \tag{4}$$

The round-trip retardation (φ_{s2}) of the sample can be calculated with

$$\varphi_{s2} = 2\cos^{-1}\left\{\frac{1}{2}\,\frac{|\mathrm{tr}\,\mathbf{J}_{s2} + \det\mathbf{J}_{s2}/|\det\mathbf{J}_{s2}|\mathrm{tr}\,\mathbf{J}_{s2}{}^{*}|}{[\mathrm{tr}(\mathbf{J}_{s2}{}^{*}\mathbf{J}_{s2}) + 2|\det\mathbf{J}_{s2}|]^{1/2}}\right\}, \tag{5}$$

or, in the case of negligible diattenuation in the sample, by $\varphi_{s2} = 2\cos^{-1}\{[J_{s2}(1,1) + J_{s2}(2,2)]/2\}$.

We can also prove from Eq. (2) that the elements of $\mathbf{J}_{fc1}$ are real numbers and that $J_{fc1}{}^{2}(1,1) + J_{fc1}{}^{2}(1,2) = 1$. Consequently, we can introduce a new parameter γ as follows:

$$\mathbf{J}_{fc1} = \begin{bmatrix} \cos\gamma & \sin\gamma \\ -\sin\gamma & \cos\gamma \end{bmatrix}. \tag{6}$$

$\mathbf{J}_{fc1}$ thus represents a rotation matrix. In other words, the Jones matrix of the sampling fiber is decomposed into a linear retarder and a rotator because $\mathbf{J}_{f1} = \mathbf{J}_{fc1}\mathbf{J}_{fl1}$. Equation (4) is equivalent to rotating the fast axis of $\mathbf{J}_{s2}$ along the axis of the incident light by an angle γ. This rotation does not affect the amplitudes of either the birefringence or diattenuation. As a result, the calibrated round-trip retardation of the sample can be calculated exactly from Eq. (5). From Eqs. (4) and (6), we can calculate the calibrated orientation of birefringence as follows:

$$\theta_{s2} = \theta_{sc2} - \gamma\,, \tag{7}$$

where θ_{sc2} can be calculated from the fast eigenvector of $\mathbf{J}_{sc2}$.

The calibration in Eq. (7) has an offset γ that depends on the parameters of the sampling fiber only. This offset is a constant in an image frame as long as the parameters of the sampling fiber are kept constant during the image acquisition of each frame, which is the case when the fast lateral scanning of OCT does not move the sampling fiber. Therefore, a relative distribution of the orientation of the birefringence can be retrieved. If the parameters of the sampling fiber are varied among the A scans, which is true when the lateral scanning in OCT does move the sampling fiber, γ will differ among the A lines. In this case, if the orientation of the birefringence of the surface layer is constant or known *a priori*, or if a known thin retarder is attached to the sample as the first layer, γ can be eliminated. In either case, φ_{s2} can be calculated exactly.

Figure 1 shows a schematic of the experimental system. The two source beams (superluminescent diodes; central wavelength $\overline{\lambda} = 850$ nm, FWHM bandwidth $\Delta\lambda = 26$ nm), one amplitude modulated at 3 kHz and the other at 3.5 kHz, are merged by a polarizing beam splitter (PBS1). Both the sample and the reference beams are coupled into a 0.5-m-long single-mode fiber. A 45° linear polarizer is used to control the polarization state of the reference beam. The horizontally (H) and vertically (V) polarized components of the interference signal are detected by photodiodes PDH and PDV, respectively. The data processing and the Jones matrix calculation were described previously.[4,5]

We first tested the system by imaging a quarter-wave ($\lambda/4$) plate in combination with a mirror, for a

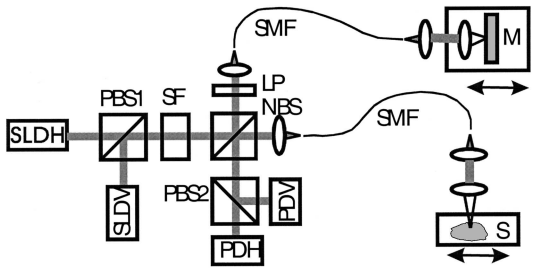

Fig. 1. Schematic of the fiber-based Mueller OCT system. SLDH and SLDV, superluminescent diodes, H and V polarized, respectively; PBS1 and PBS2, polarizing beam splitters; SF, spatial filter assembly; LP, linear polarizer; NBS, nonpolarizing beam splitter; M, mirror; SMFs, single-mode optical fibers; PDH and PDV, photodiodes for the H and V polarization components, respectively.

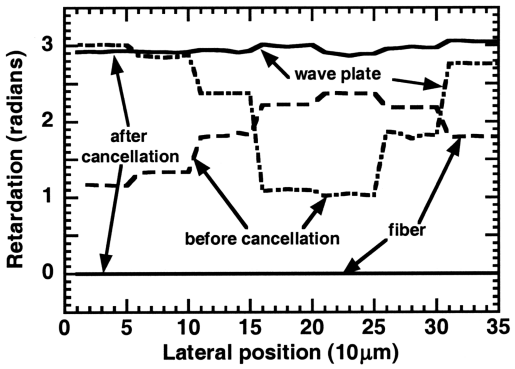

Fig. 2. Round–trip phase retardation of a $\lambda/4$ plate calculated from the measured Jones matrix before and after cancellation of the polarization distortion caused by the sampling optical fiber. The phase retardation of the sampling fiber, which is by definition zero after cancellation, is shown as well.

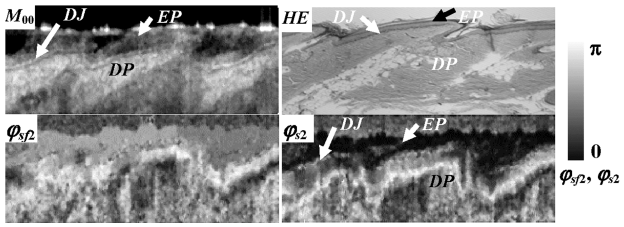

Fig. 3. M_{00} image of the Mueller matrix, the retardation images before and after cancellation of the polarization effect of the sampling fiber φ_{sf2} and φ_{s2} of the skin of a rat tail measured with the fiber-based Mueller OCT system. A histological image stained with hematoxylin and eosin is also shown for comparison. The M_{00} image is on a logarithmic scale, and the retardation images are on a linear scale. The height of each image is 1 mm. EP, epidermis; DP, dermal papilla; DJ, dermal–epidermal junction.

frame consisting of 35 A scans with a lateral span of 1 mm. The sampling fiber was intentionally deformed every fifth A scan to vary its polarization property. In Fig. 2, one can see that the raw round-trip retardation of the $\lambda/4$ plate was severely distorted by the sampling fiber. The measured $\mathbf{J}_{f2}$ was used to cancel the distortion with the algorithm described in Eqs. (2) and (3). The calibrated φ_{s2} of the $\lambda/4$ plate shown in Fig. 2 accurately matches the expected value of the half-wave, indicating the validity of our algorithm.

We then used the fiber-based Mueller OCT system to image a biological sample, the skin of a rat tail (Berlin Drucrey). After the hair of the tail was removed with hair remover lotion, the tail was scrubbed with glycerin. Two-dimensional data of the skin were taken by lateral movement of the sample between A scans. The sampling fiber was intentionally disturbed between A scans to introduce distortions. The Jones matrix was calibrated pixelwise and then converted into its corresponding 4×4 Mueller matrix.[4,5] Figure 3 shows the images of the polarization-independent M_{00} element of the Mueller matrix, the retardation before calibration (φ_{sf2}), and the retardation after calibration (φ_{s2}). Some structures, such as the dermal–epidermal junction and the collagen-rich dermal papillae, can be clearly seen in the M_{00} and φ_{s2} images, whereas they are blurred in the φ_{sf2} image because of the distortion of the sampling fiber. Also shown in Fig. 3 is the hematoxylin and eosin histological image of the tail skin of the same breed. The calibrated OCT images conform well with the histological image.

In conclusion, single-mode optical fibers have successfully been incorporated into our Mueller OCT system. A rigorous algorithm was invented to precisely eliminate the polarization effect of the sampling fiber on the retardation image of a sample dynamically. With this algorithm, the distribution of the orientation of the birefringence can also be extracted with only a constant offset in each pixel as long as the sampling fiber is not scanned during the acquisition of each image frame. Our fiber-based Mueller OCT system was successfully applied to imaging of biological samples.

Thanks to Geng Ku for assistance in machining mechanical components for this study. This project was sponsored in part by National Institutes of Health grants R21 EB00319-02 and R01 EB000712, by National Science Foundation grant BES-9734491, and by Texas Higher Education Coordinating Board grant 000512-0063-2001. L. V. Wang's e-mail address is lwang@tamu.edu.

References

1. J. F. de Boer, T. E. Milner, M. J. C. van Gemert, and J. S. Nelson, Opt. Lett. **22,** 934 (1997).
2. G. Yao and L.-H. V. Wang, Opt. Lett. **24,** 537 (1999).
3. S. Jiao, G. Yao, and L.-H. V. Wang, Appl. Opt. **39,** 6318 (2000).
4. S. Jiao and L.-H. V. Wang, Opt. Lett. **27,** 101 (2002).
5. S. Jiao and L.-H. V. Wang, J. Biomed. Opt. **7,** 350 (2002).
6. Y. Yasuno, S. Makita, Y. Suto, M. Itoh, and T. Yatagai, Opt. Lett. **27,** 1803 (2002).
7. C. E. Saxer, J. F. de Boer, B. H. Park, Y. Zhao, Z. Chen, and J. S. Nelson, Opt. Lett. **25,** 1355 (2000).
8. S. Y. Lu and R. A. Chipman, J. Opt. Soc. Am. A **11,** 766 (1987).